Copy 204

RM E58A23

NACA RM E58A23

RESEARCH MEMORANDUM

PERFORMANCE OF A 28-INCH RAMJET UTILIZING GASEOUS HYDROGEN AT A MACH NUMBER OF 3.6, ANGLES OF ATTACK UP TO 12°, AND PRESSURE ALTITUDES UP TO 110,000 FEET

By Norman T. Musial, James J. Ward, and Joseph F. Wasserbauer

Lewis Flight Propulsion Laboratory
Cleveland, Ohio

NATIONAL ADVISORY COMMITTEE FOR AERONAUTICS

WASHINGTON

May 19, 1958

Reclassified May 29, 1959

[redacted]

NACA RM E58A23

NATIONAL ADVISORY COMMITTEE FOR AERONAUTICS

RESEARCH MEMORANDUM

PERFORMANCE OF A 28-INCH RAMJET UTILIZING GASEOUS HYDROGEN AT A MACH NUMBER OF 3.6, ANGLES OF ATTACK UP TO 12°, AND PRESSURE ALTITUDES UP TO 110,000 FEET

By Norman T. Musial, James J. Ward, and Joseph F. Wasserbauer

12712

SUMMARY

An investigation was conducted in the NACA Lewis 10- by 10-foot supersonic wind tunnel to evaluate the performance of a shrouded injector burner with perforated domes employed in a 28-inch ramjet using gaseous hydrogen as fuel. Steady-state data were obtained at a pressure altitude of 77,000 feet and zero angle of attack. Transient data were obtained at pressure altitudes up to 110,000 feet and angles of attack up to 12°.

Results of this investigation showed that burning could be initiated under severe distortion conditions and that satisfactory combustor operation was accomplished up to a pressure altitude of 110,000 feet with no adverse effect on combustion efficiency. Shortening the combustion chamber decreased the combustion efficiency at the higher equivalence ratios.

INTRODUCTION

Analytical investigations of gaseous hydrogen (ref. 1) have indicated that its high flame speeds and high heating values make it desirable as a fuel for both turbojets and ramjets. The use of this fuel permits increased range both through its higher heating value and through reductions in engine weight that result from shortening the combustion chamber (ref. 2).

Research with a full-scale combustor in a connected-pipe facility (ref. 3) and with a full-scale ramjet at a Mach number of 3.0 (ref. 4) demonstrated the applicability of hydrogen as a fuel. Further research (ref. 5) on a ramjet burner at simulated altitudes approaching 120,000 feet indicated satisfactory performance. The full-scale data of reference 4, however, is limited to altitudes of about 70,000 feet, while the direct connected-pipe tests of reference 5 at higher altitudes are not full-scale and entail virtually distortion-free operation.

*Title, Unclassified.

Therefore, a full-scale investigation utilizing hydrogen at extremely high altitudes and high distortion was conducted in the Lewis 10- by 10-foot supersonic wind tunnel with a 28-inch ramjet. The ramjet engine incorporated a flameholder of the design reported in reference 5 and was tested with two combustor lengths and two nozzle contraction ratios. The investigation was made at a free-stream Mach number of 3.6, angles of attack up to 12°, and pressure altitudes up to 110,000 feet.

SYMBOLS

The following symbols are used in this report:

F_n	internal force, lb
f	fuel-air ratio
M	Mach number
m	mass flow (ρAv)
P	total pressure
$\frac{P_{max} - P_{min}}{P_{av}}$	flow-distortion parameter
p	static pressure
r	radius to each total tube at rake station (model station 101.0), measured from model centerline
r_{max}	maximum radius of model
T	total temperature
W_f	fuel flow, lb/sec
η_B	combustion efficiency
τ	total-temperature ratio, T_6/T_3
φ	equivalence ratio, ratio of f to stoichiometric f

Subscripts:

av	average
max	maximum
min	minimum

[redacted]

3	diffuser exit station (model station 129.15)
6	nozzle-throat or -exit station

APPARATUS

An aft view of the 28-inch ramjet engine, installed in the 10- by 10-foot supersonic wind tunnel is presented in figure 1. The engine was strut-mounted from the top of the tunnel. The supersonic diffuser had a 20°-35° double-cone spike (fig. 2(a)) and was designed so that the two oblique shocks generated by the spike would coalesce at the cowl lip at a Mach number of 3.3. Spike translation permitted near-optimum inlet operation at Mach numbers other than design. The internal cowl-lip angle was 28.3° and the cowl projected frontal area was 11 percent of maximum. A bypass door located at model station 69.3 was positioned to bleed approximately 4 percent of the inlet mass flow via a ram scoop located on the spike shoulder (fig. 2(b)). The ram scoop is of the design reported in reference 6.

Internal pressure instrumentation consisted of a total-pressure survey with six 9-tube rakes, eight static taps, and a slotted orifice (ref. 7) at model station 101.0. In addition, as indicated in figure 2(a), static-pressure taps were located along the combustion-chamber wall. During steady-state burning operation, exit total pressure was measured at the throat of the choked nozzle by a water-cooled tail rake.

During transient engine operation, pressure variations were sensed by dynamic pickups and recorded on an oscillograph equipped with galvanometers having natural frequencies of 200 cycles per second. The tail-rake total-pressure tubes were manifolded to a pressure transducer. Tailpipe static pressure (measured at station 170.0), normal-shock-position sensing pressure (station 1.0), and diffuser-exit total pressure (measured by a slotted orifice at station 101.0) were also sensed by pressure transducers and recorded.

Four engine configurations, A, B, C, and D were investigated during the test and are outlined in the following table:

Configuration	Nozzle contraction ratio	Dome hole size, in.	Combustion-chamber length, in.
A	0.55	3/8	50.6
B	.55	3/8	26.6
C	.55	1/4	50.6
D	.70	1/4	50.6

[redacted]

Figure 2(a) also indicates the relative combustion-chamber lengths and exhaust-nozzle contraction ratios used. Combustion-chamber length, measured from the point of fuel injection to the exit nozzle throat, was nominally maintained at 50.6 inches except for configuration B, which utilized a 26.6-inch chamber. Two convergent nozzles with contraction ratios of 0.55 and 0.70 were used.

The burner configurations investigated were based on the design of burner 3 in reference 4, with the addition of perforated domes to the upstream ends of the fuel-injector shrouds. Airflow through the perforated domes was varied by enlarging the holes from a 1/4-inch diameter (3.3 percent of annular flow area of the burner) to a 3/8-inch diameter (7.7 percent of the annular flow area). A photograph of the 1/4-inch-diameter-hole burner configuration is presented in figure 3(a), while figure 3(b) shows the 3/8-inch-diameter-hole configuration.

Figure 4 shows the pilot system. To insure ignition at high altitudes, a jet of hydrogen was injected into the spark gap through a hollow electrode. The pilot fuel injector in the center of the assembly supplied the fuel that carried the flame to the burner.

A schematic diagram of the fuel system used during the test is presented in figure 5. The fuel was gaseous hydrogen supplied in cylinders at a pressure of 2400 pounds per square inch. For steady-state burning operation, the fuel was taken directly from the storage cylinder through a metering orifice and throttling valve to the engine. The pressure differential across the fuel metering orifice was measured by a mercury U-tube manometer. During transient burning operation, the throttling valve was positioned by the air pressure in the loading tank. The pressure varied nearly linearly with time because the air entered the tank through a choked orifice. Fuel-flow information was obtained by recording the pressure differential across the fuel metering orifice and the fuel valve position.

PROCEDURE

Steady-state burning data were obtained for each configuration at zero angle of attack and a pressure altitude of 77,000 feet by operating the tunnel on the propulsion cycle. At each value of fuel-air ratio designated, conditions were stabilized for approximately 2 minutes before data were taken.

Transient data were obtained for configurations A and B at angles of attack from 0° to 12° and pressure altitudes of 77,000 to 110,000 feet by operating the tunnel on the closed-loop cycle. Inasmuch as the products of combustion are not exhausted while testing in this manner, approximately 20 seconds of transient operation were available before the tunnel dewpoint became excessive. The following procedure was followed in obtaining transient data:

[redacted]

(1) The pilot was lit.

(2) The engine fuel flow was varied by increasing the loading tank pressure linearly from zero to the pressure corresponding to the highest equivalence ratio desired in a time of 10 to 20 seconds.

(3) The fuel system was shut down, and air was purged from tunnel until the measured dewpoint reached $-15^{\circ} \pm 5^{\circ}$ F.

Combustion efficiency in both cases (steady-state and transient operation) was calculated from the enthalpy rise of the gas divided by the available heat content of the fuel. The exit total temperature was obtained from the exit total pressure by using continuity relations In calculations involving transient data, exit total pressure was measured directly or determined from tailpipe static pressure by means of a calibration obtained during steady-state burning. Values used for enthalpy, ratio of specific heats, and gas constant were obtained from reference 8. Combustion-efficiency calculations for the transient data were somewhat less accurate than those for the steady-state data because of the complex method necessarily employed in obtaining transient data.

Inlet pressure recovery and distortion were obtained from the total-pressure survey at model station 101.0. The inlet mass-flow ratio was computed from the static- and total-pressure survey at this station and a calibration constant determined from cold-flow operation.

RESULTS AND DISCUSSION

Inlet Performance

Inlet performance as determined from cold-flow operation is presented in figure 6. The inlet exhibited approximately 11 counts of subcritical stability at zero angle of attack; the maximum pressure recovery was approximately 51 percent. Subcritical stability fell to 7 counts at 12° angle of attack. No apparent change in the total-pressure recovery and mass-flow characteristics due to altitude variation is indicated.

Since the inlet was initially designed for shock-on-lip operation at a free-stream Mach number of 3.3, inlet operation at a Mach number of 3.6 resulted in a spillage loss of approximately 5 percent of the total mass flow. Ram-scoop bleed on the spike shoulder accounted for approximately another $2\frac{1}{2}$ percent of the mass flow. Because of the spillage loss, the additive drag coefficient at critical inlet operation was

[redacted]

0.185; this value is based on the maximum area and determined by the method outlined in reference 9. Cowl-pressure-drag coefficient, also based on maximum area and calculated from the experimental pressure distribution along the cowl surface, was 0.045.

Diffuser-flow distortion measured at the mass-flow rake station (model station 101.0) is presented in figure 7. Flow distortion increases rapidly with increasing angle of attack, as indicated in figure 7(a). There is no appreciable difference in the flow distortion at zero angle of attack for burning or cold-flow operation (fig. 7(b)). Velocity profiles presented in figure 8 correspond to the points of distortion for the highest M_3 at each angle of attack in figure 7(a). As angle of attack is increased, peak velocities in the upper half of the duct shift toward the centerbody; and the flow in the lower half of the duct approaches separation. The profiles at zero angle of attack are representative of the diffuser conditions under which steady-state burning operation was initiated.

Steady-State Burning Performance

Steady-state burning performance for the burners of this investigation and for burner 3 of reference 4 are given in figure 9. Although burner 3 of reference 4 maintained a high level of combustion efficiency over a relatively large range of equivalence ratios, the efficiency decreased rapidly below an equivalence ratio of 0.275. In an effort to improve the combustion efficiency at these low values of equivalence ratio, domes were attached to the upstream ends of the shrouds enclosing the fuel-injector bars, as reported in reference 5. The purpose of the domes was to improve lean fuel-air ratio operation and to insure ignition at high altitudes by providing a local fuel-rich mixture in the vicinity of the injector bars.

The performance curve for configuration C indicates that the addition of domes with 1/4-inch-diameter holes resulted in improved efficiency at low equivalence ratios, as compared with burner 3 of reference 4. The over-all efficiency level, however, was somewhat lower than anticipated, based on the data of reference 5. Operation with a larger exit nozzle (configuration D) and somewhat higher equivalence ratios also resulted in low combustion efficiency.

An increase in dome flow area (3/8-inch-diameter holes, configuration A) resulted in a much higher level of combustion efficiency, with a gradual decrease in efficiency with increasing equivalence ratios. In order to improve combustion efficiency at high equivalence ratios, it appears that a further increase of airflow through the domes would be desirable.

[redacted]

The effect of combustion-chamber length on combustor performance is presented in figure 9(b). The combustion efficiency decreased rapidly as equivalence ratio increased when the combustion chamber was shortened 2 feet. Static-pressure taps located along the combustor indicated that burning was not complete in the 26.6-inch length. The burner of this investigation was affected more by shortening the tailpipe than the 16-inch-diameter engine of reference 4.

Figure 10 shows the net internal specific impulse obtained with configuration A (convergent nozzle), to indicate the order of magnitude obtained. The dashed curve is the calculated net internal specific impulse for 100-percent combustion efficiency, based on the diffuser pressure recovery of the data of configuration A. In both cases, external drag is not included.

Transient Burning Performance

A transient trace, typical of those used for obtaining combustion efficiencies, is presented in figure 11. At point 0, the fuel valve opens and fuel is admitted to the burner. At point 1, corresponding to an equivalence ratio of 0.103, burner ignition is indicated by a rise in the tail-rake total and tailpipe static pressure. The sharp rise in tail-rake total and tailpipe static pressure between points 1 and 4 indicates a sharp rise in combustion efficiency in this region. The rise in normal-shock-sensing static pressure at point 14 indicates the inlet approaching critical operation.

The effect of altitude on combustion efficiency at zero angle of attack for two engine configurations is given in figures 12 and 13. The burner ignited at all times at zero angle of attack and at pressure altitudes up to 110,000 feet. The combustion-chamber static pressure prior to ignition at an altitude of 110,000 feet was about 80 millimeters of mercury or approximately 1/10 atmosphere. Ignition could not be attained at a combustion-chamber static pressure of 50 millimeters of mercury (altitude, 120,000 ft).

Performance curves for configuration A (50.6-inch combustion chamber length) presented in figure 12 indicate satisfactory combustor performance is possible at the pressure altitudes investigated. As altitude increased, the equivalence ratio necessary for high efficiency operation increased steadily until, at an altitude of 110,000 feet, an equivalence ratio of 0.250 was necessary to attain practical efficiencies. Altitude effect on configuration B (26.6-inch combustion chamber length) at pressure altitudes up to 100,000 feet is given in figure 13. Again, data indicate that the combustor performance is satisfactory throughout the altitude range and that the equivalence ratio must be increased with altitude for efficient burning. The data, however, are in closer agreement with

[redacted]

steady-state burning data than for configuration A. In general, the level of combustion efficiency is not adversely effected by increasing pressure altitude. The points numbered on the figure correspond to the points indicated on the trace of figure 11.

It was possible to ignite the burner for configurations A and B at angles of attack of 6° and 12° at pressure altitudes as high as 100,000 feet. For these conditions, inlet distortion before ignition would be as high as 68 percent, as indicated in figures 7 and 8. Combustion efficiencies obtained for these traces are similar to those at zero angle of attack and are not presented.

The inlet air temperature during burning operation was 750° R compared with 1410° R, which would be obtained in flight at the same Mach number and altitude. Because of this lower air temperature, combustion severity at an altitude of 110,000 feet in the 10- by 10-foot tunnel is approximately the same as at 118,000 feet in flight, as calculated from the severity parameter of reference 10.

SUMMARY OF RESULTS

The following results were obtained during a study of the internal performance of a 28-inch ramjet using gaseous hydrogen as a fuel at Mach number 3.6 in the NACA Lewis 10- by 10-foot supersonic wind tunnel:

1. Data indicate that burning was initiated under severe distortion conditions and that satisfactory combustor operation was accomplished up to a pressure altitude of 110,000 feet at zero angle of attack. Burning was also accomplished at angles of attack up to 12° at pressure altitudes up to 100,000 feet.

2. Effect of altitude on the level of combustion efficiency appeared to be negligible; however, as altitude was increased, the equivalence ratio necessary for efficient burning also increased.

3. Perforated domes attached to the shrouds of the burner resulted in improved operation at low equivalence ratios.

4. Shortening the combustion chamber decreased the combustion efficiency at the higher equivalence ratios.

Lewis Flight Propulsion Laboratory
National Advisory Committee for Aeronautics
Cleveland, Ohio, February 4, 1958

[redacted]

REFERENCES

1. Silverstein, Abe, and Hall, Eldon W.: Liquid Hydrogen as a Jet Fuel for High-Altitude Aircraft. NACA RM E55C28a, 1955.

2. Cervenka, A. J., and Sheldon, J. W.: Method for Shortening Ram-Jet Engines by Burning Hydrogen Fuel in the Subsonic Diffuser. NACA RM E56G27, 1956.

3. Dangle, E. E., and Kerslake, William R.: Experimental Evaluation of Gaseous Hydrogen Fuel in a 16-Inch-Diameter Ram-Jet Engine. NACA RM E55J18, 1955.

4. Wasserbauer, Joseph F., and Wilcox, Fred A.: Combustor Performance of a 16-Inch Ram Jet Using Gaseous Hydrogen as Fuel at Mach Number 3.0. NACA RM E56K28a, 1957.

5. Kerslake, William R.: Combustion of Gaseous Hydrogen at Low Pressures in a 35° Sector of a 28-Inch-Diameter Ramjet Combustor. NACA RM E58A21a, 1958.

6. Connors, James F., Wise, George A., and Lovell, J. Calvin: Investigation of Translating-Double-Cone Axisymmetric Inlets with Cowl Projected Areas 40 and 20 Percent of Maximum at Mach Numbers from 3.0 to 2.0. NACA RM E57C06, 1957.

7. Whalen, Paul P., and Wilcox, Fred A.: Use of Subsonic Diffuser Mach Number as a Supersonic-Inlet Control Parameter. NACA RM E56F05, 1956.

8. English, Robert E., and Hauser, Cavour H.: Thermodynamic Properties of Products of Combustion of Hydrogen with Air for Temperatures of 600° to 4400° R. NACA RM E56G03, 1956.

9. Sibulkin, Merwin: Theoretical and Experimental Investigation of Additive Drag. NACA Rep. 1187, 1954. (Supersedes NACA RM E51B13.)

10. Childs, J. Howard: Preliminary Correlation of Efficiency of Aircraft Gas-Turbine Combustors in Different Operating Conditions. NACA RM E50F15, 1950.

CI-2

[redacted]

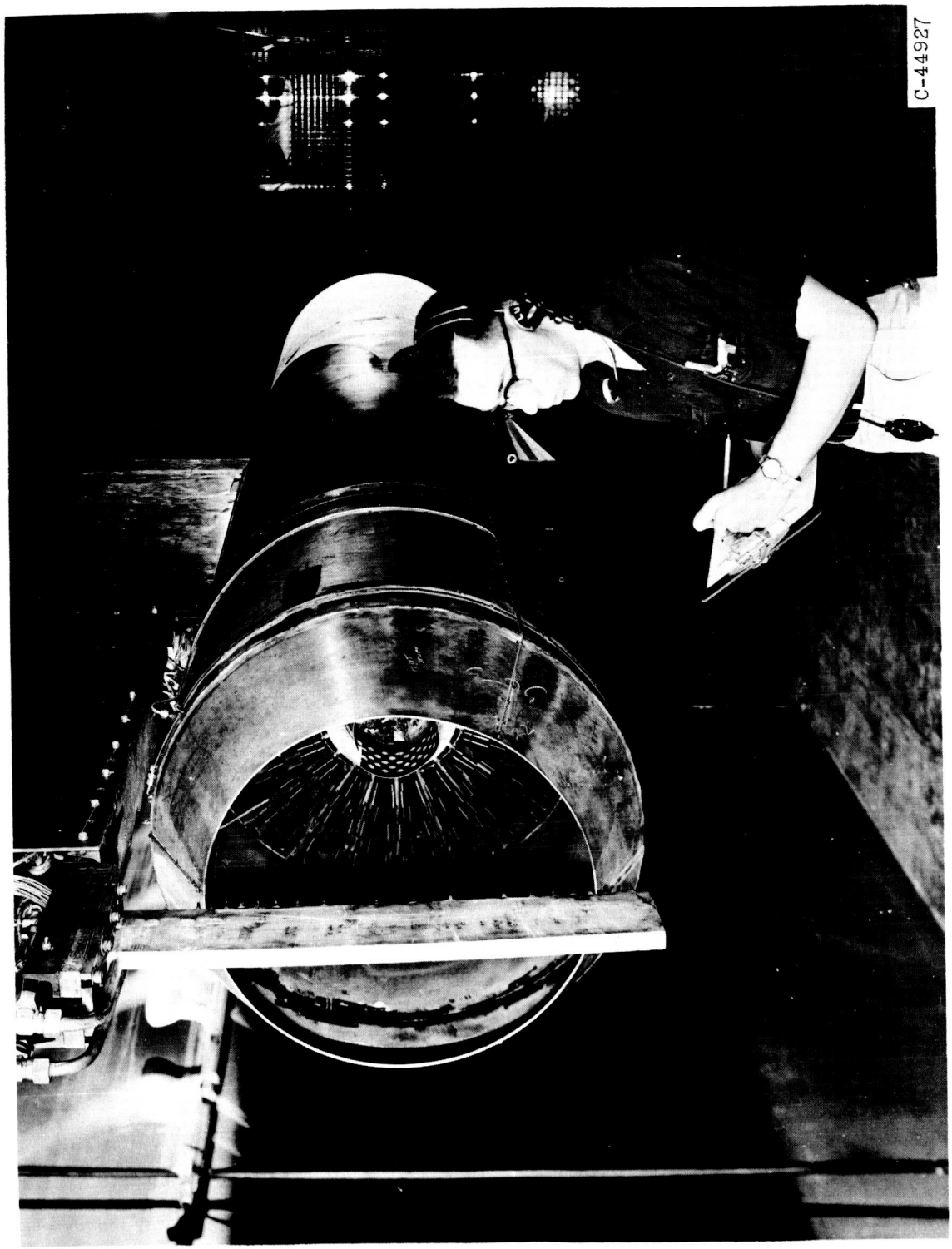

Figure 1. - Rear view of 28-inch ramjet installed in 10- by 10-foot tunnel.

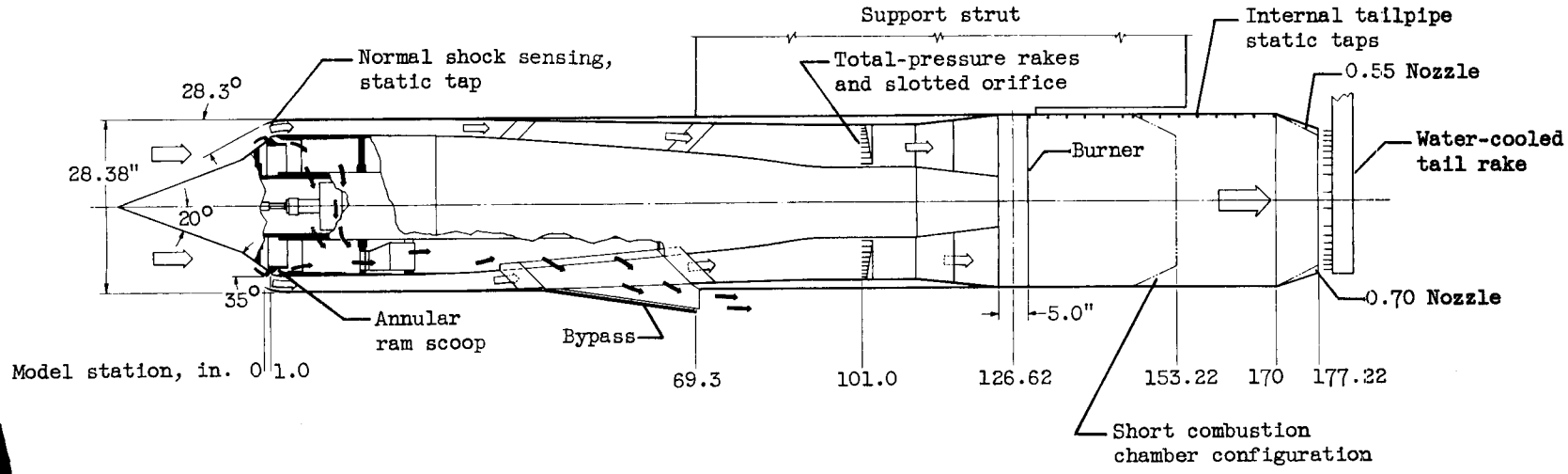

(a) Basic engine configuration.

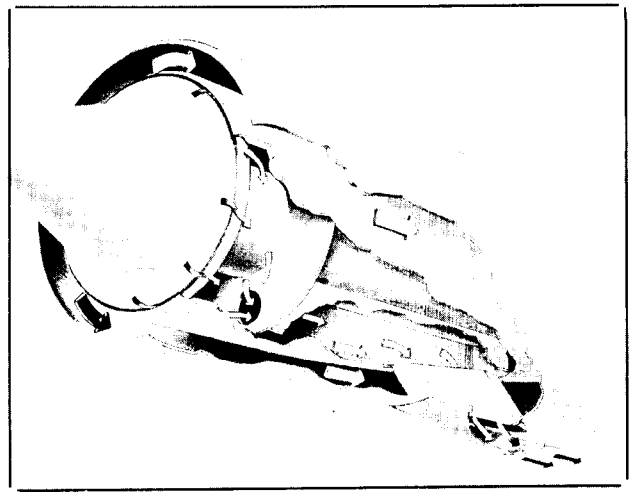

CD-6025

(b) Detail of annular ram scoop and bypass.

Figure 2. - Schematic diagram of 28-inch diameter ramjet engine.

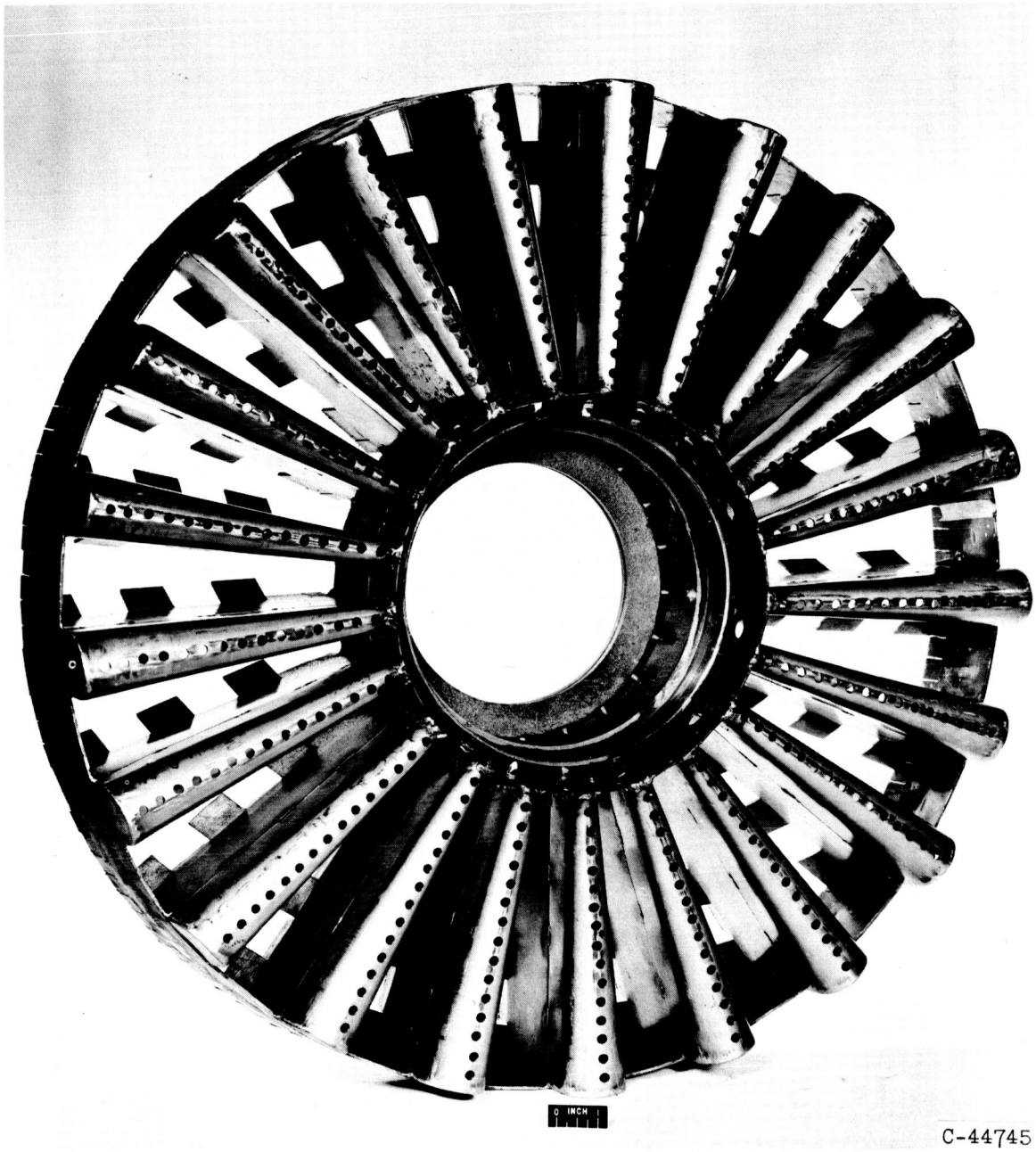

(a) 1/4-Inch-diameter-hole configuration.

Figure 3. - Front view of flameholder.

[redacted]

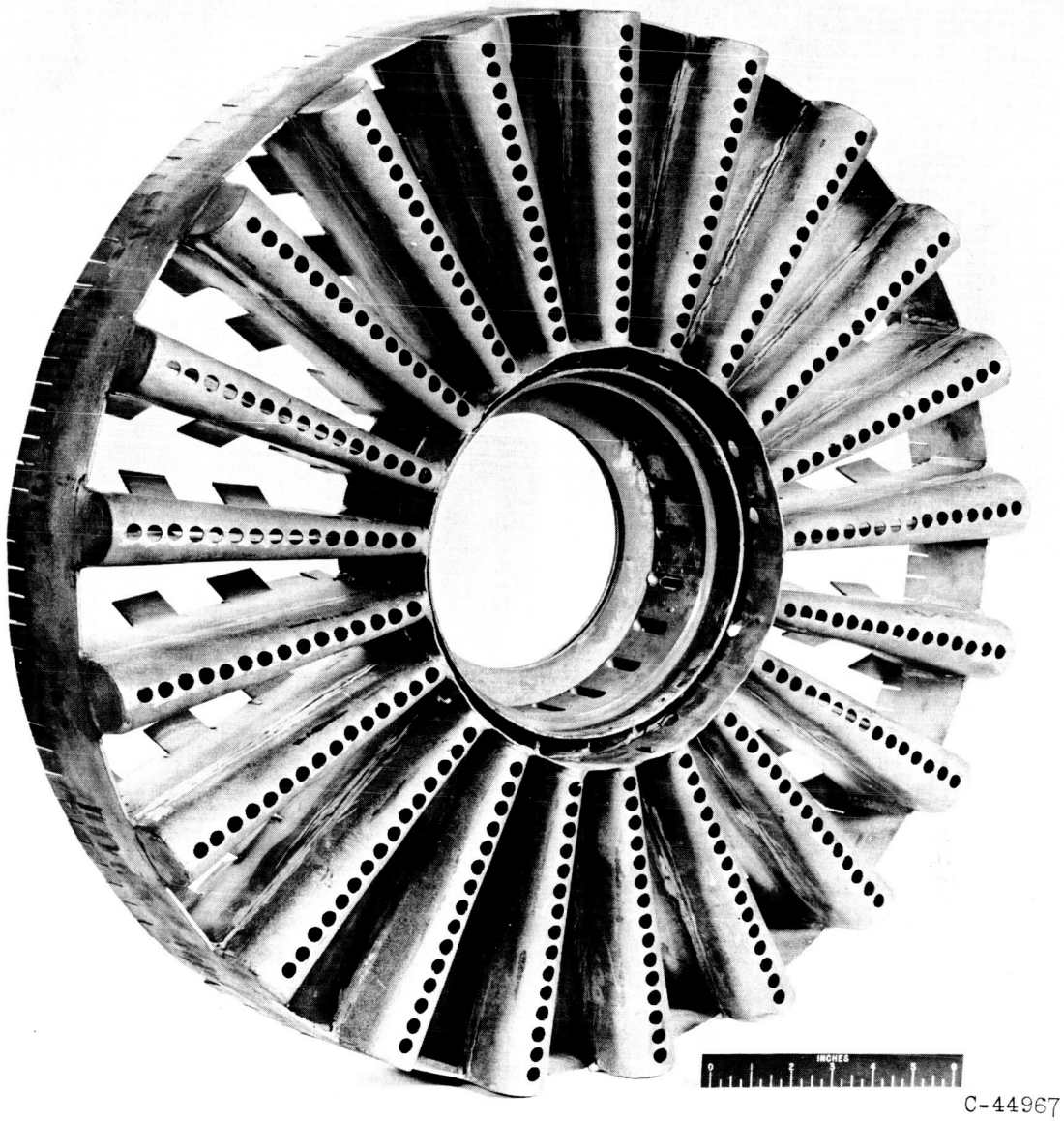

(b) 3/8-Inch-diameter-hole configuration.

Figure 3. - Concluded. Front view of flameholder.

[redacted]

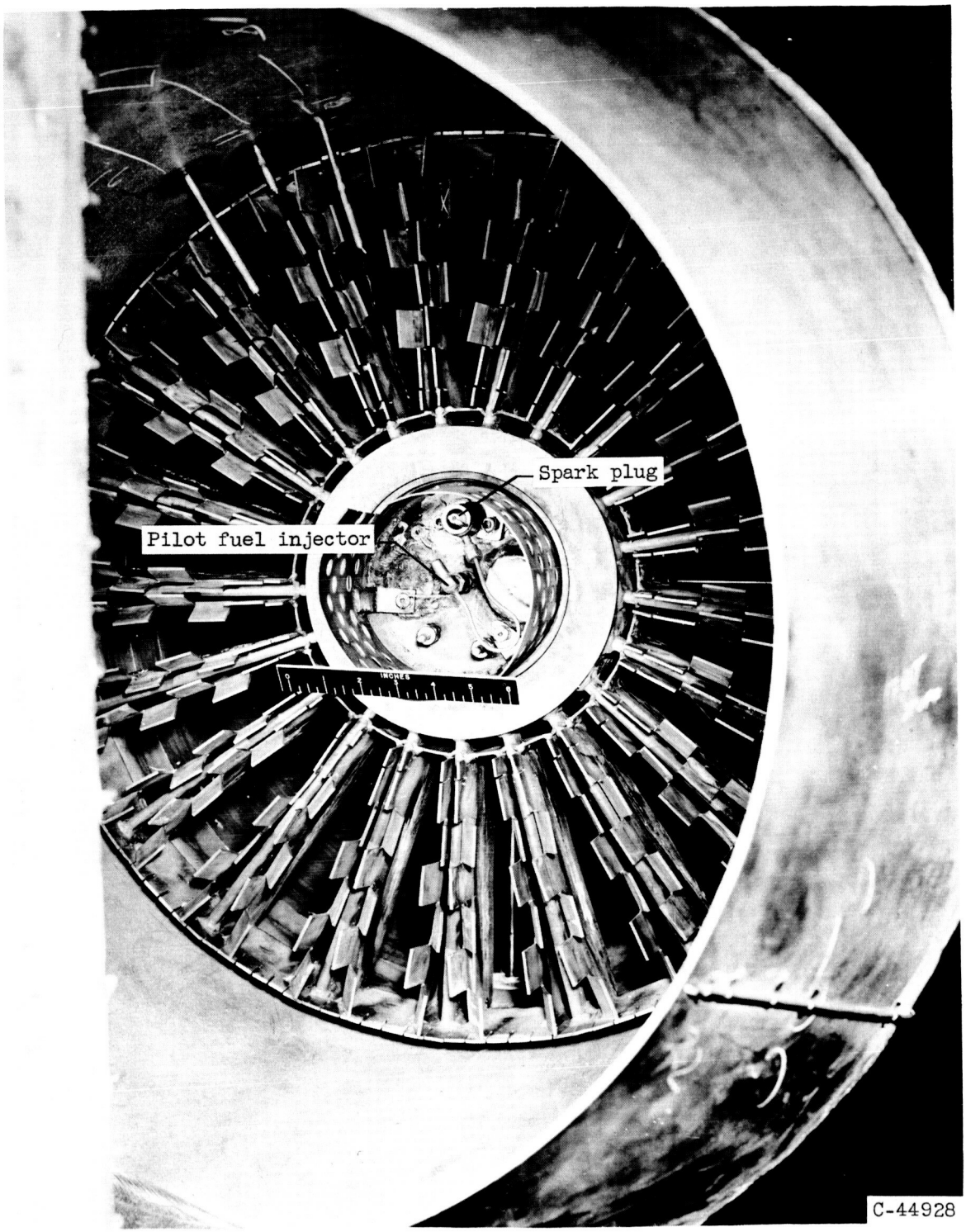

Figure 4. - Rear view of flameholder showing pilot configuration.

[redacted]

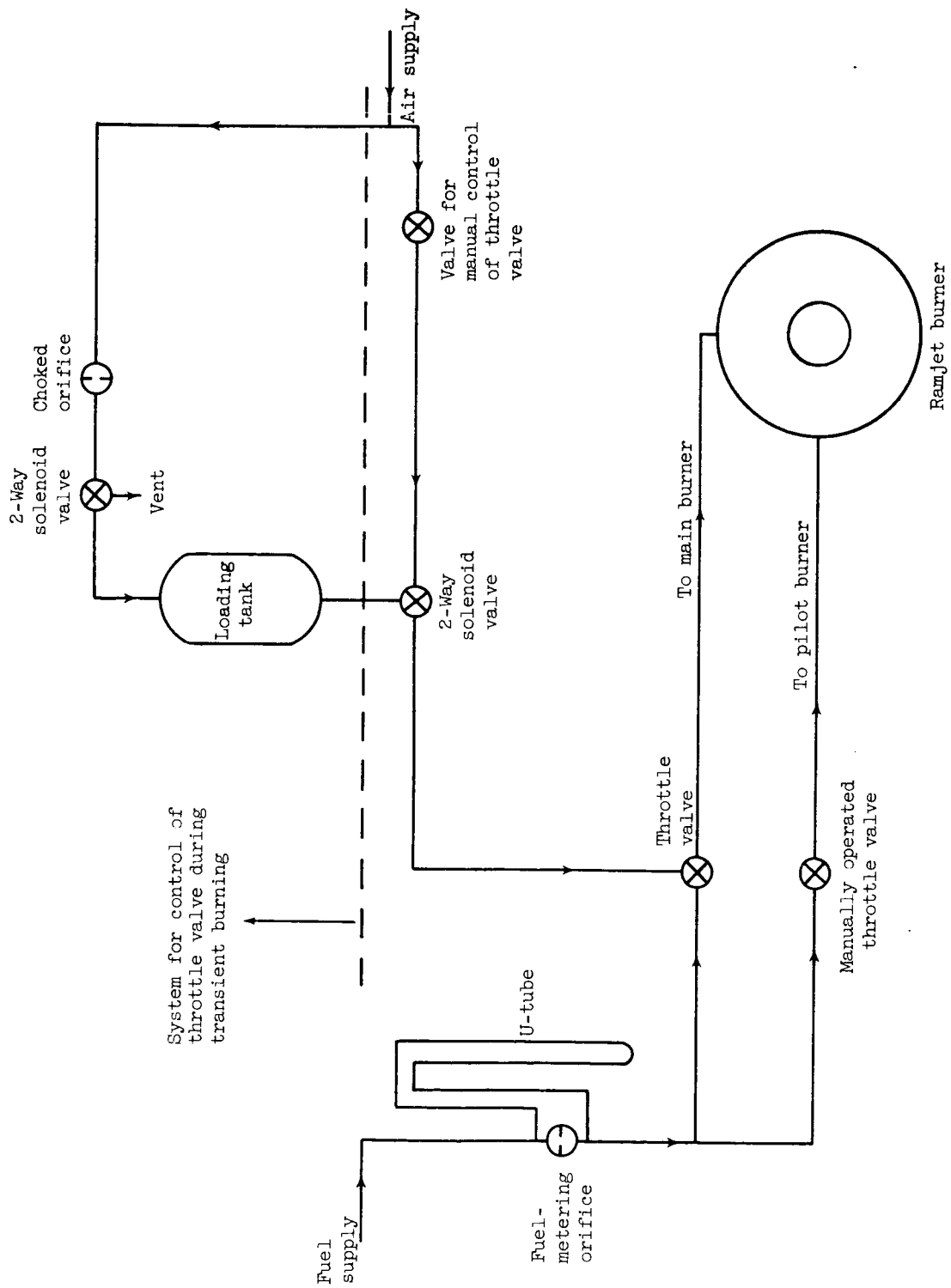

Figure 5. - Fuel system.

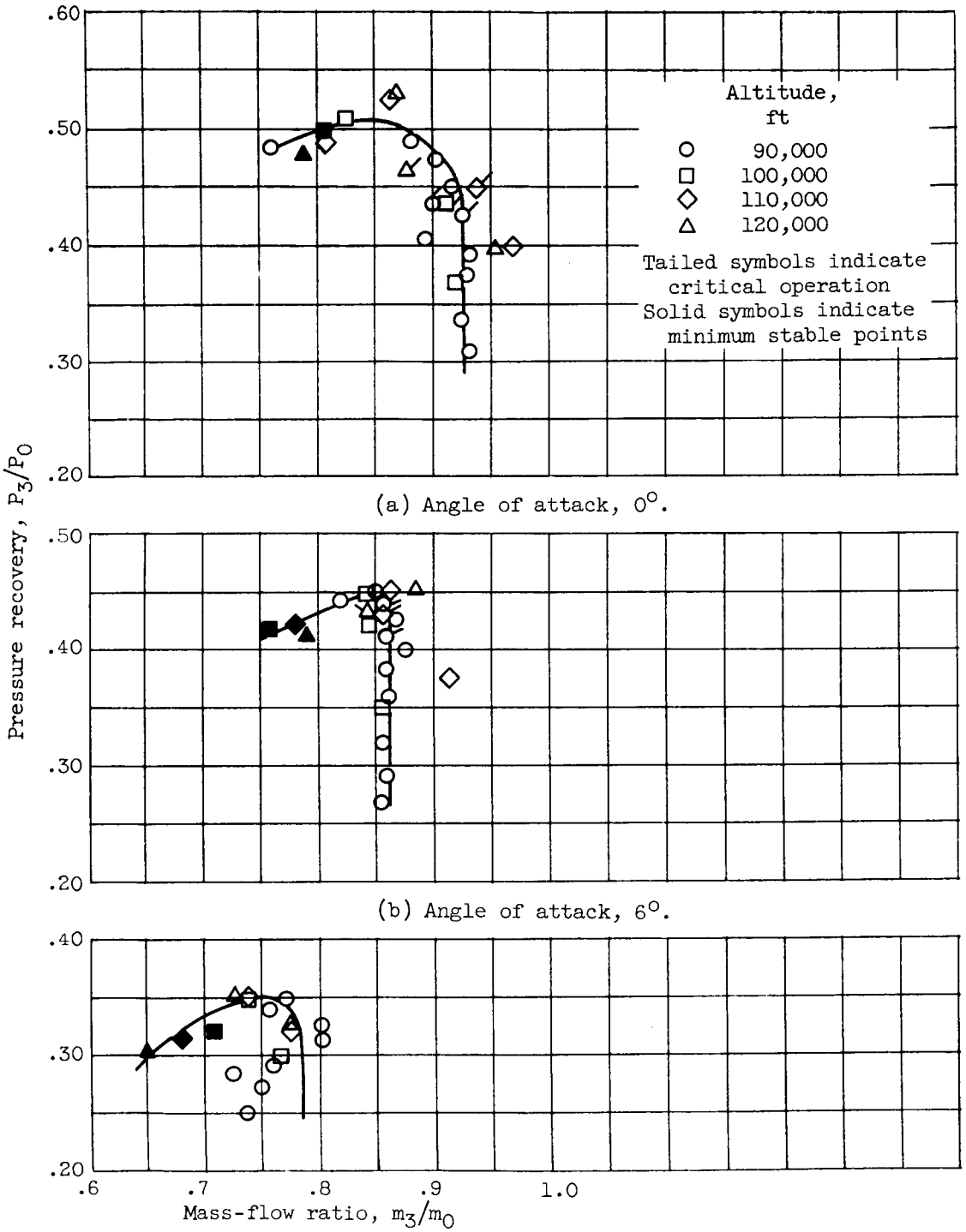

(a) Angle of attack, 0°.

(b) Angle of attack, 6°.

(c) Angle of attack, 12°.

Figure 6. - Diffuser performance characteristics at a Mach number of 3.6.

[redacted]

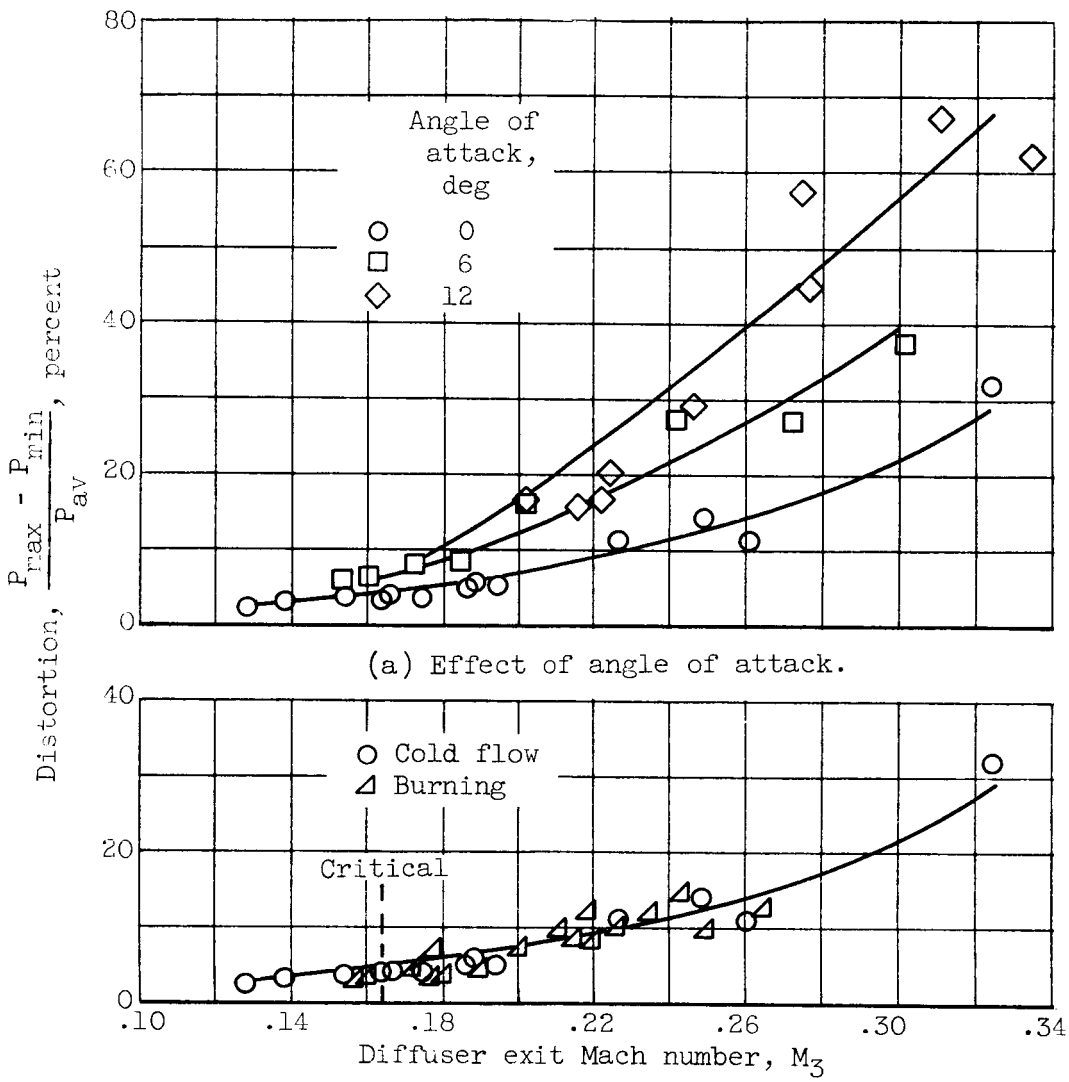

(a) Effect of angle of attack.

(b) Effect of burning; angle of attack, 0°.

Figure 7. - Inlet distortion characteristics.

CJ-3

[redacted]

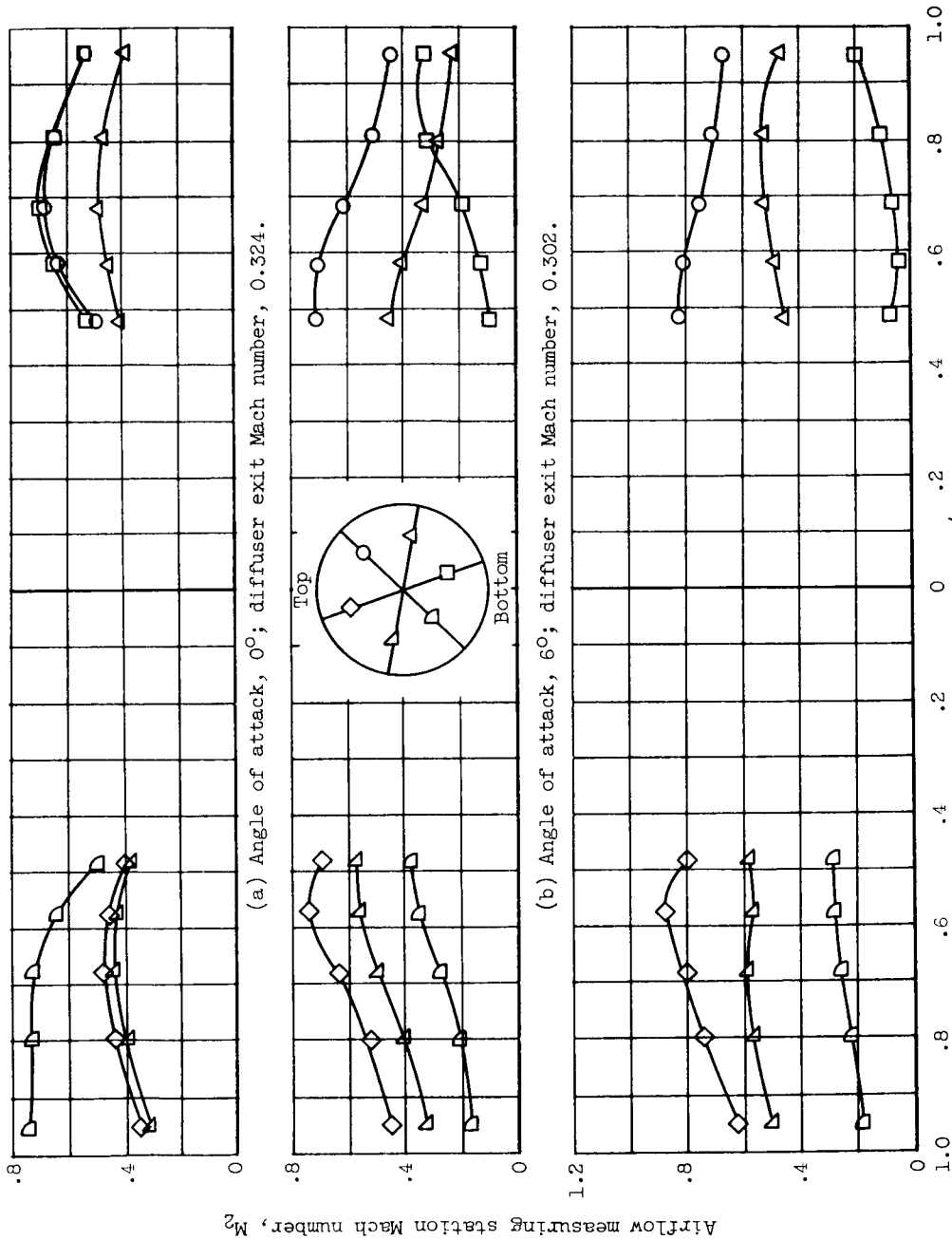

Figure 8. - Profiles of diffuser-discharge Mach number at angles of attack up to 12°.

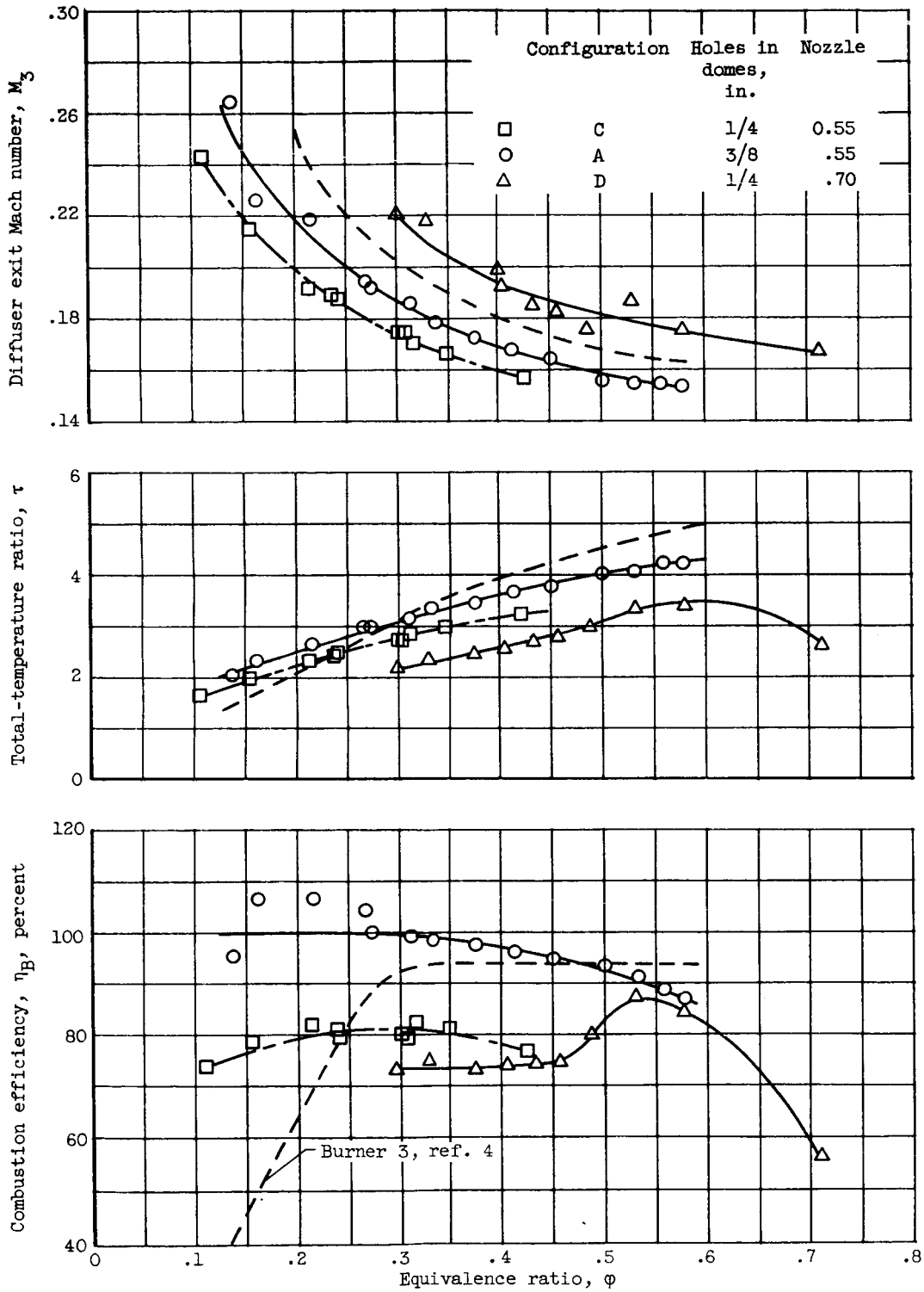

(a) Effect of dome hole size and nozzle size on combustor performance.

Figure 9. - Steady-state combustor performance. Angle of attack, 0°; altitude, 77,000 feet.

[redacted]

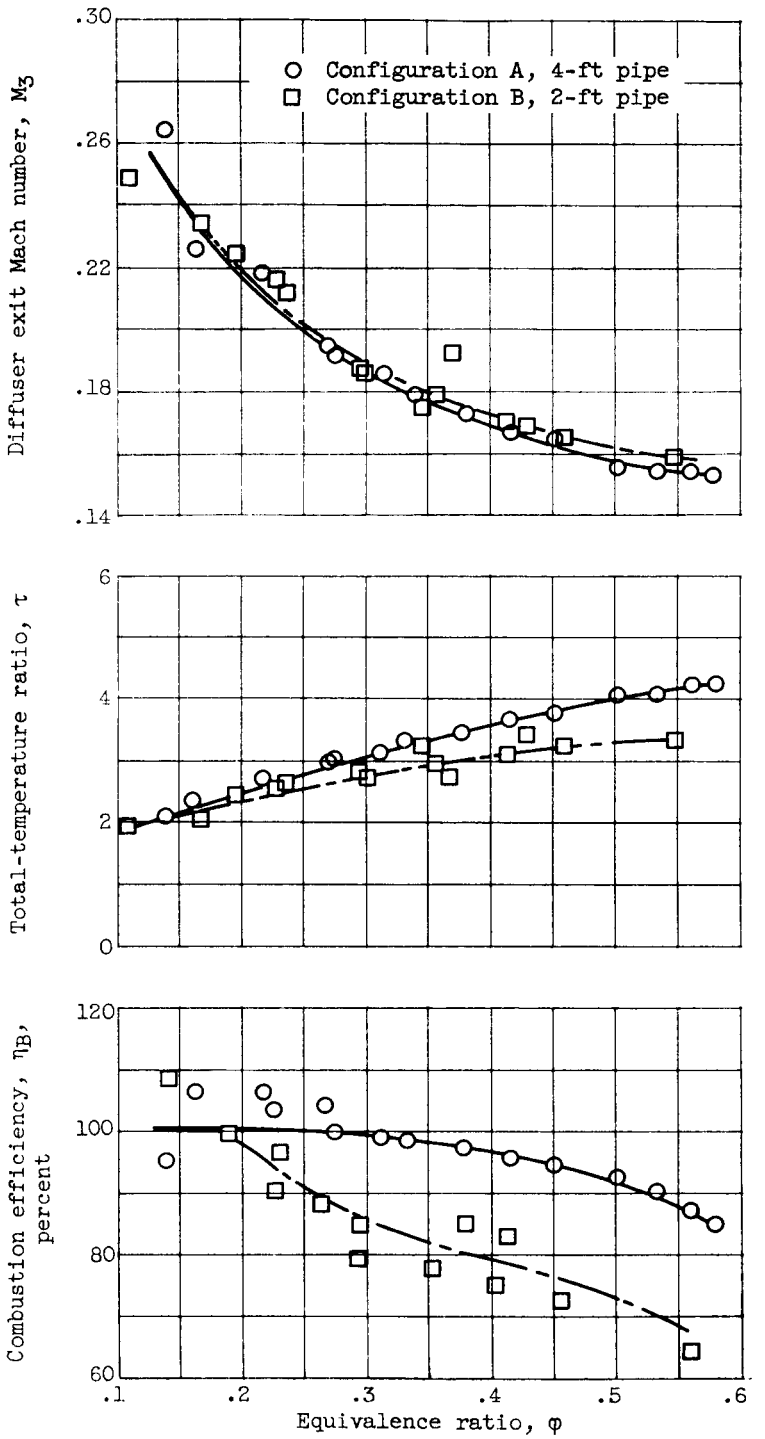

(b) Effect of combustion-chamber length on combustor performance.

Figure 9. - Concluded. Steady-state combustor performance. Angle of attack, 0°; altitude, 77,000 feet.

[redacted]

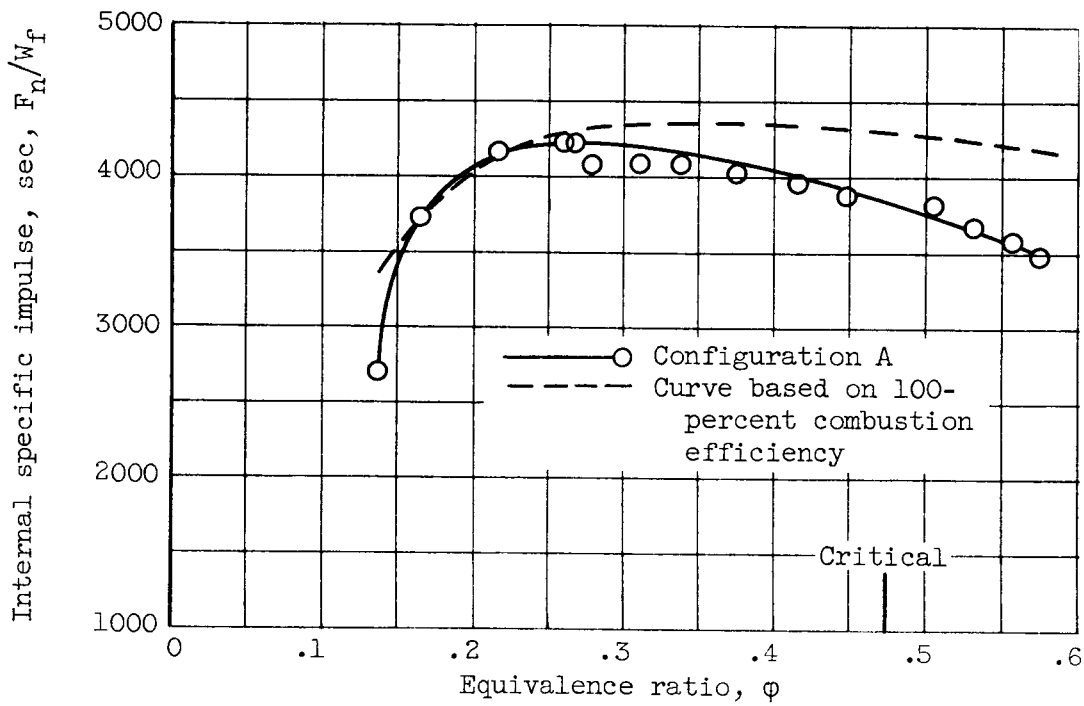

Figure 10. - Comparison of calculated specific impulse based on 100-percent combustion efficiency with experimental data of configuration A.

[redacted]

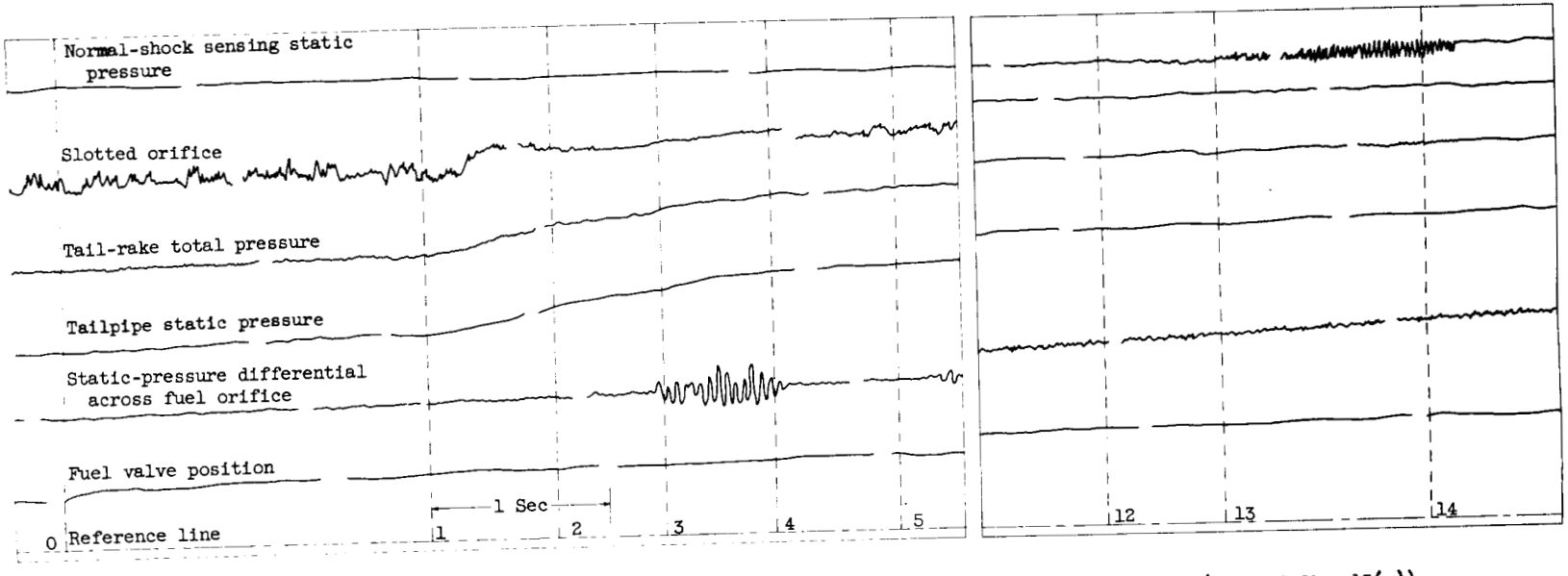

Figure 11. - Trace of configuration B operation at 100,000-foot altitude and zero angle of attack (data of fig. 13(c)).

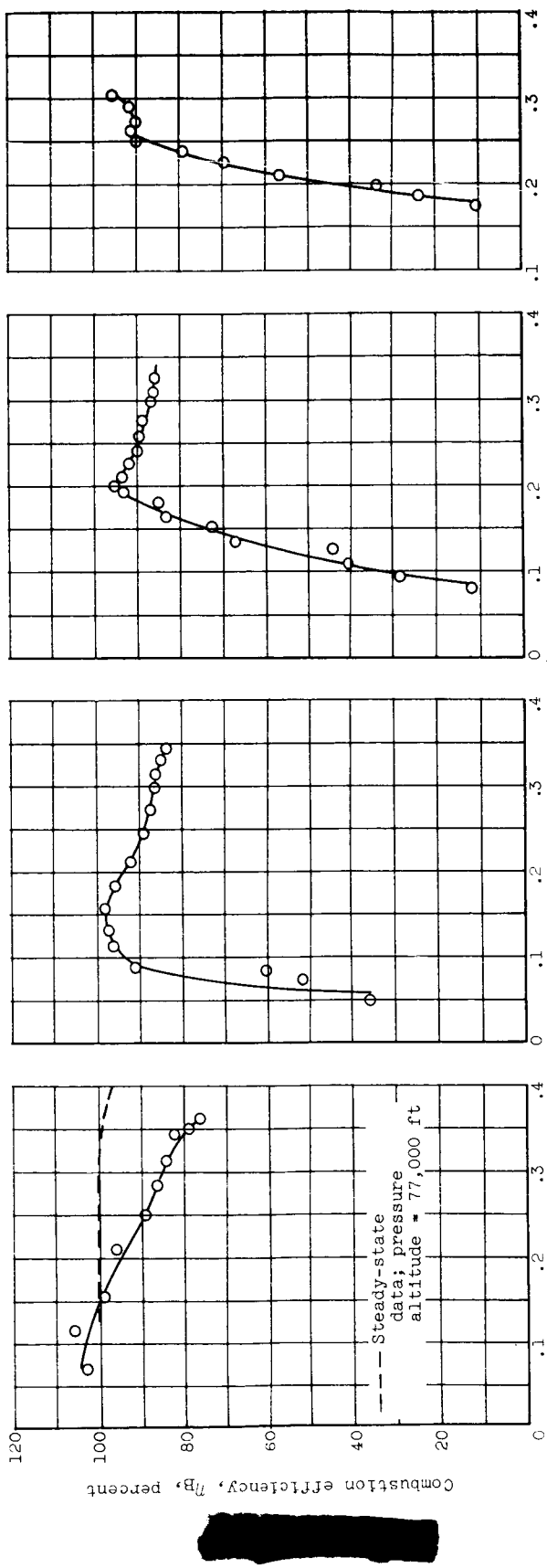

(a) Pressure altitude, 80,000 feet.

(b) Pressure altitude, 90,000 feet.

(c) Pressure altitude, 100,000 feet.

(d) Pressure altitude, 110,000 feet.

Figure 12. - Altitude effect on combustion efficiency of configuration A at zero angle of attack.

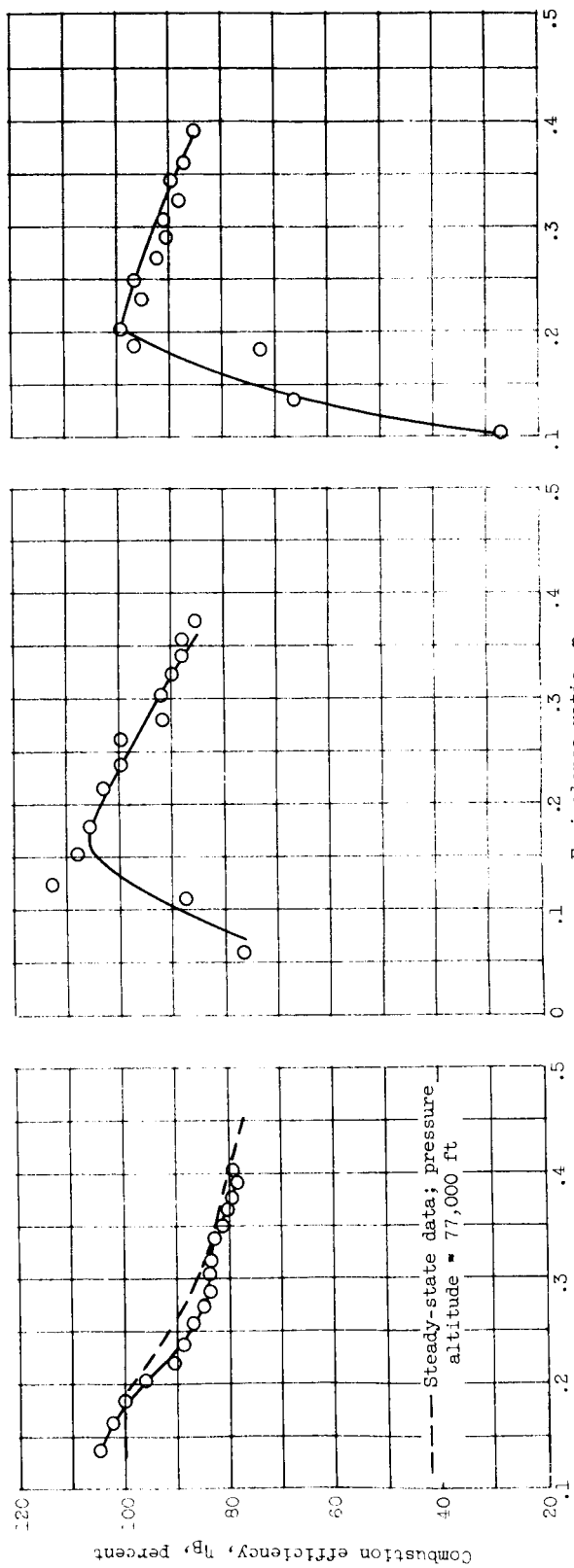

(a) Pressure altitude, 80,000 feet.

(b) Pressure altitude, 90,000 feet.

(c) Pressure altitude, 100,000 feet.

Figure 13. - Altitude effect on combustion efficiency of configuration B at zero angle of attack.